Nonequilibrium dielectric behavior in glasses at low temperatures: Evidence for interacting defects

Hervé M. Carruzzo*
Physics Department, University of Illinois at Urbana-Champaign, 1110 West Green Street, Urbana, Illinois 61801

Eric R. Grannan† and Clare C. Yu
Department of Physics, University of California, Irvine, Irvine, California 92717
(Received 17 March 1994; revised manuscript received 16 May 1994)

We find that recent low-temperature nonequilibrium dielectric experiments indicate that glasses have strongly interacting defects. While many of the features found in the experiments can be explained by the standard model of noninteracting two-level systems, we find that the frequency dependence cannot. Using a Monte Carlo simulation of a nearest-neighbor Ising spin glass, we show that interactions between defects can qualitatively explain the experiments because they lead to the formation of clusters and a hole in the distribution of local fields.

I. INTRODUCTION

The low-temperature properties of glasses, such as the specific heat and the thermal conductivity, have been traditionally explained by the model of two-level systems (TLS) which are usually thought of as tunneling centers.[1,2] The standard model of two-level systems assumes for the most part that the TLS do not interact with one another. Recently, however, several groups have suggested that interaction between defects may be crucial to our understanding of the universal properties seen in amorphous materials.[3–7] Unfortunately, since both interacting and noninteracting models have been able to explain the low-temperature experiments, there has been no way of clearly determining whether or not interactions between defects are truly important. This absence of a definitive experimental test may be due to the fact that most experiments on amorphous materials are equilibrium measurements.

Recently, however, B. Tigner *et al.* at Stanford have undertaken nonequilibrium dielectric experiments which show that interactions do indeed play an important role in the low-temperature physics of glasses. They have discovered unexpected behavior in the dielectric properties of glasses such as SiO_2, SiO_x ($x \simeq 2.1$), and polymers.[8] Using an ac capacitance bridge, they have been studying the history-dependent dielectric constant of 1–3 μm films of glass samples at temperatures between 20 and 1000 mK. The amplitude of the ac fields range from 1×10^3 to 5×10^5 V/m at frequencies between 1 and 10 kHz. After the sample is cooled, a large dc field ($\sim10^6-10^7$ V/m) is applied. As a result, the capacitance jumps up and then decays logarithmically with time. (They also find that the resistance, which is out of phase with the ac signal, jumps up and decays logarithmically with time.) After applying a fixed voltage for some time (a day), they subsequently sweep the dc bias field and find that a hole has formed in the capacitance at the previously applied bias voltage. In the absence of an applied field they find a hole at zero bias. They have also examined the temperature and ac frequency dependence of the slope of the logarithmic time decay ($dC/d\ln t$, where C is capacitance).[9] They find that the magnitude of the slope, as well as the size of the jump, decreases with increasing temperature and increasing frequency.

To understand this behavior, we can start by asking the following question. To what extent can these experiments be explained by the standard model of noninteracting two-level systems? As we shall see in Sec. II, the jump in the capacitance and its subsequent logarithmic decay is consistent with the model of noninteracting TLS. In addition, the decrease in the magnitude of the slope of the logarithmic decay with increasing temperature is also consistent with noninteracting TLS. However, the standard model predicts that the slope of the logarithmic decay will be independent of frequency because the frequency is much smaller than the effective TLS energy splitting. This lack of frequency dependence contradicts experiment. This leads us to consider interactions between defects mediated by the strain field. In Sec. III we identify two important consequences of interactions: (1) a hole in the distribution of local electric fields seen by single dipoles; and (2) clusters of strongly interacting defects. We have studied these effects using a Monte Carlo simulation of a three-dimensional nearest-neighbor Ising spin glass, and we find qualitative agreement with experiment. In Sec. IV we argue that clusters are crucial to the understanding of the frequency dependence seen in the experiments. In particular, we include the time-dependent hole in the density of states at low energies in calculating the capacitance due to TLS. We find that the resulting frequency dependence is much smaller than that seen experimentally. This implies that even single TLS with a density of states that include correlations are insufficient to explain the experiments and hence, that clusters play an important role in glasses. In using the term "cluster", we are referring to a group of defects with collective excitations which result from correlations.

II. NONINTERACTING TWO-LEVEL SYSTEMS

We consider a two-level system that is sitting in a double-well potential with an asymmetry energy Δ, and a

tunneling matrix element Δ_0 describing transitions between the wells. The Hamiltonian is[1]

$$H_0=\frac{1}{2}\begin{bmatrix}\Delta & \Delta_0\\ \Delta_0 & -\Delta\end{bmatrix}. \tag{1}$$

When the external dc and ac fields are applied, they will affect the energy asymmetry of the wells. Thus

$$H_{\rm dc}=\begin{bmatrix}1 & 0\\ 0 & -1\end{bmatrix}\mathbf{p}\cdot\mathbf{E}_{\rm dc} \tag{2}$$

and

$$H_{\rm ac}=\begin{bmatrix}1 & 0\\ 0 & -1\end{bmatrix}\mathbf{p}\cdot\mathbf{E}_{\rm ac}(t), \tag{3}$$

where $\mathbf{p}$ is the electric dipole moment of the two-level system, $\mathbf{E}_{\rm dc}$ is the external dc electric field, $\mathbf{E}_{\rm ac}(t)=\mathbf{E}_{\rm ac}\cos\Omega t$ is the small perturbing ac field, and Ω is the ac frequency. It is convenient to diagonalize $H_0+H_{\rm dc}$ and treat $H_{\rm ac}$ as the perturbing Hamiltonian. In this new basis the Hamiltonian becomes

$$H=\frac{1}{2}\begin{bmatrix}\tilde{\epsilon} & 0\\ 0 & -\tilde{\epsilon}\end{bmatrix}+\begin{bmatrix}\tilde{\Delta}/\tilde{\epsilon} & \Delta_0/\tilde{\epsilon}\\ \Delta_0/\tilde{\epsilon} & -\tilde{\Delta}/\tilde{\epsilon}\end{bmatrix}\mathbf{p}\cdot\mathbf{E}_{\rm ac}(t)\ , \tag{4}$$

where $\tilde{\Delta}=\Delta+2\mathbf{p}\cdot\mathbf{E}_{\rm dc}$ and $\tilde{\epsilon}=\sqrt{\tilde{\Delta}^2+\Delta_0^2}$. In this new basis, the dc field and the energy splitting of the two-level system will produce an effective field along the z axis, while the ac field will be in the x-z plane at some angle to the z axis. Notice, however, that $\mathbf{E}_{\rm dc}$ now has x and z components. This implies that the polarization will also have x and z components. When the dc field is first applied, the two-level systems will be out of thermal equilibrium in terms of the population of the levels. They will equilibrate in a characteristic time τ_1. If we think of the two-level systems as spins, then we can say that the z component aligns with the total field in a characteristic time τ_1. Notice that the dynamics of this system can be described with the Bloch equations of motion that are familiar from NMR.[10,11] According to these equations, if a spin is not aligned along the field, then it will precess about the total field.

Let us first consider an elementary example in which a spin $\mathbf{S}$ precesses around an effective field $\mathbf{B}=\mathbf{B}_0+\mathbf{B}_1\cos\Omega t$ where the static field $\mathbf{B}_0$ points along the z axis and the time-dependent field points along the x axis.[11] If we momentarily ignore the relaxation terms, then the equation for precession is simply:

$$\frac{d\mathbf{S}}{dt}=\gamma\mathbf{S}\times\mathbf{B}\ , \tag{5}$$

where γ is the gyromagnetic ratio. If we transform to the frame which rotates about the z axis with frequency Ω, then there is a component of the ac field which is static and points along the new x' axis. In this frame the equation of motion is

$$\frac{d\mathbf{S}}{dt}=\mathbf{S}\times[(\omega_0-\Omega)\hat{z}+\omega_1\hat{x}'], \tag{6}$$

where $\omega_0=\gamma B_0$ and $\omega_1=\gamma B_1$. Notice that even if the ac field is far from resonance, we will get a response in phase with the ac field proportional to B_1. It is the analog of this response which contributes to the measured capacitance.

Now let us include the relaxation times and write down the Bloch equations:[11,12]

$$\frac{dS_x}{dt}-\gamma(S_yB_z-S_zB_y)+\frac{1}{\tau_2}S_x=0\ , \tag{7}$$

$$\frac{dS_y}{dt}-\gamma(S_zB_x-S_xB_z)+\frac{1}{\tau_2}S_y=0\ , \tag{8}$$

$$\frac{dS_z}{dt}-\gamma(S_xB_y-S_yB_x)+\frac{1}{\tau_1}(S_z-\langle S_z\rangle)=0\ , \tag{9}$$

where the spin $\mathbf{S}=\boldsymbol{\sigma}/2$, $\boldsymbol{\sigma}$ is a vector of Pauli matrices, and τ_2 is the transverse dephasing time due to spin-spin interactions. $\langle S_z\rangle$ is the thermal equilibrium value of S_z, and is given by $\langle S_z\rangle=\tanh(\beta\gamma\hbar B_z(t)/2)/2$ where $\beta=1/kT$. The effective magnetic field is $\mathbf{B}=\mathbf{B}_{\rm dc}+\mathbf{B}_{\rm ac}$ where $-\hbar\gamma\mathbf{B}_{\rm dc}=(0,0,\tilde{\epsilon})$ and

$$-\hbar\gamma\mathbf{B}_{\rm ac}/2=(\Delta_0/\tilde{\epsilon},0,\tilde{\Delta}/\tilde{\epsilon})p_0E_{\rm ac}\cos\theta\cos\Omega t\ .$$

Here p_0 is the magnitude of the dipole moment, and θ is the angle between the dc field and the dipole moment.

Since the perturbing ac field is a small perturbation, we can linearize the Bloch equations by only keeping terms to first order in $B_{\rm ac}$. This means that we expand $\langle S_z\rangle=\tanh(\beta\gamma\hbar B_z(t)/2)/2$ in a Taylor series, and we look for solutions to the Bloch equations of the form $\mathbf{S}(t)=\mathbf{S}^0(t)+\mathbf{S}^1(t)$, where $\mathbf{S}^0(t)=(0,0,S_z^0(t))$ is zeroth order in $B_{\rm ac}$ and $\mathbf{S}^1(t)$ is first order in $B_{\rm ac}$. Thus the linearized Bloch equations become

$$\frac{dS_z^0}{dt}+\frac{1}{\tau_1}[S_z^0(t)-S_z^0(\infty)]=0\ , \tag{10}$$

$$\frac{dS_x^1}{dt}-\omega_0S_y^1+\frac{1}{\tau_2}S_x^1=0\ , \tag{11}$$

$$\frac{dS_y^1}{dt}+\omega_0S_x^0+\frac{1}{\tau_2}S_y^1-\delta\alpha S_z^0(t)\cos\Omega t=0\ , \tag{12}$$

$$\frac{dS_z^1}{dt}+\frac{1}{\tau_1}(S_z^1-\delta\lambda\cos\Omega t)=0\ , \tag{13}$$

where the resonance frequency $\omega_0=\gamma B_{z,\rm dc}=-\tilde{\epsilon}/\hbar$, $\delta=-(2\tilde{\Delta}/\hbar\tilde{\epsilon})p_0E_{\rm ac}\cos\theta$ is first order in $E_{\rm ac}$, the equilibrium value of the aligned spin $S_z^0(\infty)=-\tanh(\beta\tilde{\epsilon}/2)/2$, $\alpha=\Delta_0/\tilde{\Delta}$, and $\lambda=\hbar\beta[1-4(S_z^0(\infty))^2]/4$. If we introduce raising and lowering operators $S^{\pm}=S_x^1\pm iS_y^1$, then the equations for S^+ and S^- separate. The equation for S^+ becomes

$$\frac{dS^+(t)}{dt}+i\left(\omega_0-\frac{i}{\tau_2}\right)S^+(t)-i\alpha\delta S_z^0(t)\cos\Omega t=0 \tag{14}$$

and the equations for S^- is the complex conjugate of this.

It is straightforward to write down the solutions of these equations.

$$S_z^0(t)=S_z^0(\infty)+[S_z^0(0)-S_z^0(\infty)]e^{-t/\tau_1}\ , \tag{15}$$

$$S_z^1(t)=\frac{\delta\lambda}{1+\tau_1^2\Omega^2}[\cos\Omega t+\tau_1\Omega\sin\Omega t]\ , \tag{16}$$

$$S^+(t)=\frac{\delta\alpha[(\omega_0-i/\tau_2)\cos\Omega t-i\Omega\sin\Omega t]S_z^0(\infty)}{(\omega_0-i/\tau_2)^2-\Omega^2}+\frac{\delta\alpha[(\omega_0+i/\tau_1-i/\tau_2)\cos\Omega t-i\Omega\sin\Omega t][S_z^0(0)-S_z^0(\infty)]e^{-t/\tau_1}}{(\omega_0+i/\tau_1-i/\tau_2)^2-\Omega^2}. \tag{17}$$

The equation for $S^-(t)$ is the complex conjugate of the equation for $S^+(t)$. $S_z^0(0)$ is the initial value of $S_z^0(t)$ shortly after the dc field is applied. We have ignored terms that oscillate at frequency ω_0 since we are only interested in terms that oscillate at the ac frequency. The expression for $S_z^0(t)$ shows that an individual TLS relaxes exponentially back to its equilibrium value $S_z^0(\infty)$. This exponential time dependence feeds into $S^+(t)$. When it is averaged over the TLS parameters, it will give the logarithmically slow time decay seen in the capacitance. Quantum mechanically, $S^\pm$ are raising and lowering operators that govern transitions between the two energy levels. Equation (17) indicates that the amplitude for such transitions is enhanced when the system deviates from equilibrium. This makes sense since such transitions are needed to restore equilibrium.

Now we must relate the Bloch spins to the polarization in the direction of the applied electric field. In the original basis of Eqs. (1)–(3), the dipole moment operator $\boldsymbol{\pi}$ of a TLS can be written as a product of a real-space operator ($\mathbf{p}$) and a spin-space operator (σ_z), i.e., $\boldsymbol{\pi}=\sigma_z\mathbf{p}$. Thus the Hamiltonian for coupling to an electric field is $\boldsymbol{\pi}\cdot\mathbf{E}$, where the dot product refers to real space [see Eqs. (2) and (3)]. If we transform $\boldsymbol{\pi}$ to a basis in which $H_0+H_{\rm dc}$ is diagonal as in Eqs. (1) and (2), then

$$\boldsymbol{\pi}=\left[\frac{\tilde{\Delta}}{\bar{\epsilon}}\sigma_z+\frac{\Delta_0}{\bar{\epsilon}}\sigma_x\right]\mathbf{p}. \tag{18}$$

Using $\mathbf{S}=\boldsymbol{\sigma}/2$ and $\mathbf{p}\cdot\mathbf{E}=-p_0E\cos\theta$, we see that the component $p_\parallel$ of the dipole moment along the direction of the field is given by

$$p_\parallel=-\langle\boldsymbol{\pi}\rangle\cos\theta=-p_0\cos\theta\left[\frac{2\tilde{\Delta}S_z^1(t)}{\bar{\epsilon}}+\frac{\Delta_0(S^++S^-)}{\bar{\epsilon}}\right], \tag{19}$$

where the average values $\langle\sigma_z\rangle$ and $\langle\sigma_x\rangle$ found in $\langle\boldsymbol{\pi}\rangle$ are given by the solutions to the Bloch equations.

The susceptibility is given by $\chi=\chi'+\chi''=dp_\parallel/dE_{\rm ac}$, where χ' is in phase and χ'' is out of phase with the ac signal. For convenience we write $\chi'=\chi_z'+\chi_{1\pm}'+\chi_{2\pm}'$ and $\chi''=\chi_z''+\chi_{1\pm}''+\chi_{2\pm}''$, where χ_z comes from S_z^1 in Eq. (16) and $\chi_{1,2\pm}$ from $S^\pm$ in Eq. (17). Thus

$$\chi_z'=\left[\frac{\tilde{\Delta}p_0\cos\theta}{\bar{\epsilon}}\right]^2\frac{\beta\{1-4[S_z^0(\infty)]^2\}}{1+\tau_1^2\Omega^2}\ , \tag{20}$$

$$\chi_{1\pm}'=-\frac{2}{\hbar}\left[\frac{\Delta_0p_0\cos\theta}{\bar{\epsilon}}\right]^2\times\left[\frac{\omega_0+\Omega}{1+(\omega_0+\Omega)^2\tau_2^2}+\frac{\omega_0-\Omega}{1+(\omega_0-\Omega)^2\tau_2^2}\right]\tau_2^2S_z^0(\infty)\ , \tag{21}$$

$$\chi_{2\pm}'=-\frac{2}{\hbar}\left[\frac{\Delta_0p_0\cos\theta}{\bar{\epsilon}}\right]^2\times\left[\frac{\omega_0+\Omega}{1+\tau_{12}^2(\omega_0+\Omega)^2}+\frac{\omega_0-\Omega}{1+\tau_{12}^2(\omega_0-\Omega)^2}\right]\times\tau_{12}^2[S_z^0(0)-S_z^0(\infty)]e^{-t/\tau_1}\ , \tag{22}$$

$$\chi_z''=\left[\frac{\tilde{\Delta}p_0\cos\theta}{\bar{\epsilon}}\right]^2\frac{\beta\{1-4[S_z^0(\infty)]^2\}\tau_1\Omega}{1+\tau_1^2\Omega^2}\ , \tag{23}$$

$$\chi_{1\pm}''=\frac{2}{\hbar}\left[\frac{\Delta_0p_0\cos\theta}{\bar{\epsilon}}\right]^2\times\left[\frac{1}{1+(\omega_0+\Omega)^2\tau_2^2}-\frac{1}{1+(\omega_0-\Omega)^2\tau_2^2}\right]\tau_2S_z^0(\infty), \tag{24}$$

$$\chi_{2\pm}''=\frac{2}{\hbar}\left[\frac{\Delta_0p_0\cos\theta}{\bar{\epsilon}}\right]^2\times\left[\frac{1}{1+(\omega_0+\Omega)^2\tau_{12}^2}-\frac{1}{1+(\omega_0-\Omega)^2\tau_{12}^2}\right]\times\tau_{12}[S_z^0(0)-S_z^0(\infty)]e^{-t/\tau_1}\ , \tag{25}$$

where $\tau_{12}^{-1}=\tau_2^{-1}-\tau_1^{-1}$ and $\bar{\epsilon}=-\hbar\omega_0$. Notice that only $\chi_{2\pm}'$, which is proportional to $\exp(-t/\tau_1)$, will contribute to the time-dependent capacitance.

We must average χ over the distribution of two-level systems and over the dipole orientation angle θ. The usual assumption[1] for the distribution of parameters is $P(\Delta,\tilde{\lambda})=\bar{P}$, where $\bar{P}$ is a constant and the tunneling matrix element is given by the WKB formula $\Delta_0=\hbar\omega_0\exp(-\tilde{\lambda})$. This implies that

$$P(\Delta,\Delta_0)=\frac{\bar{P}}{\Delta_0}\ . \tag{26}$$

Thus the average $\langle\chi\rangle_{\rm TLS}$ is given by

$$\langle\chi\rangle_{\rm TLS}=\frac{\bar{P}}{2}\int_{-\Delta^{\rm max}}^{\Delta^{\rm max}}d\Delta\int_{\Delta_0^{\rm min}}^{\Delta_0^{\rm max}}\frac{d\Delta_0}{\Delta_0}\int_{-1}^{1}d(\cos\theta)\chi(\Delta,\Delta_0,\cos\theta)\ , \tag{27}$$

where the factor of $\frac{1}{2}$ comes from the average over $\cos\theta$. The capacitance is then given by

$$C=\frac{A(\epsilon_0+\langle\chi'\rangle_{\rm TLS})}{d}\ , \tag{28}$$

where A is the area of the capacitor plates and d is the distance between them. ϵ_0 is the permittivity of free space.

In order to compare the calculated capacitance with experiment, we estimate the values of the parameters and do the integral in Eq. (27) numerically using Monte Carlo integration.[13] We now discuss our choice of parameters. In the standard model, an excited two-level system decays to the ground state by emitting a phonon. Thus the longitudinal relaxation rate is given by[1]

$$\tau_1^{-1}=\frac{\tilde{\gamma}^2}{\rho}\left[\frac{1}{c_l^5}+\frac{2}{c_t^5}\right]\frac{\tilde{\epsilon}^3}{2\pi\hbar^4}\left[\frac{\Delta_0}{\tilde{\epsilon}}\right]^2\coth\left[\frac{\beta\tilde{\epsilon}}{2}\right]\ , \tag{29}$$

where $\tilde{\gamma}$ is the deformation potential, ρ is the mass density, c_l is the longitudinal speed of sound, and c_t is the transverse speed of sound.

The transverse relaxation time τ_2 is the characteristic time for dephasing and spectral diffusion due to dipole-dipole interactions. Like τ_1, it has been measured in SiO_2 in phonon and electric echo experiments.[14,15] Since we are interested in the behavior of the TLS which take a long time to tunnel, we use the expression that is appropriate for times much longer than the shortest τ_1.[2] In this case τ_2 is proportional to T^{-1}. Since $\langle\chi\rangle_{\rm TLS}$ is rather insensitive to τ_2, we ignore its dependence on Δ and Δ_0, and use the experimental value:[15]

$$\tau_2\approx\frac{8\times10^{-7}}{T}\ \text{sec}\ , \tag{30}$$

where T is in Kelvin. Note that $\tau_2^{-1}\gg\Omega$ for the experimental range of temperatures.

We also need an expression for the initial value of the spin $S_z^0(0)$. When $\mathbf{E}=0$, the TLS eigenvalues are $\pm\frac{1}{2}\epsilon=\pm\frac{1}{2}\sqrt{\Delta^2+\Delta_0^2}$. Thus $S_z^0(0)=-\tanh(\beta\epsilon/2)/2$. In the adiabatic limit the eigenfunctions evolve continuously as the dc field is applied. Thus the TLS eigenvalues $+\epsilon/2$ $(-\epsilon/2)$ in the absence of an electric field become $+\tilde{\epsilon}/2$ $(-\tilde{\epsilon}/2)$ when we turn on the field. [Note that if the field is turned on instantaneously, the TLS population can be inverted due to the sudden level crossing which occurs if $(1+2\mathbf{p}\cdot\mathbf{E}_{\rm dc}/\Delta)<0$ (or equivalently if $\Delta\tilde{\Delta}<0$). In this case $S_z^0(0)=(-\tanh(\beta\epsilon/2)/2)\times{\rm sgn}(\Delta\tilde{\Delta})$. Thus, if $1+2\mathbf{p}\cdot\mathbf{E}_{\rm dc}/\Delta<0$, then $S_z^0(0)$ has the opposite sign of that found in the adiabatic limit, and the capacitance will initially jump down when the dc field is applied. Experimentally such fast switching and short observation times are very difficult to achieve, and the adiabatic limit is the correct one to choose.]

In Fig. 1(a) we have plotted the capacitance C versus $\ln t$ for various temperatures. Since all the time dependence comes from $\chi'_{2\pm}$, only this contribution to C is plotted in Fig. 1(a). We have used the values for SiO_2: $\bar{P}=10^{32}$ erg^{-1}cm^{-3}, $\tilde{\gamma}=1$ eV, $\rho=2.2$ g/cm^3, $c_l=5.8\times10^5$ cm/s, $c_t=3.8\times10^5$ cm/s, $p_0=0.5$ D, $E_{\rm dc}=2\times10^6$ V/m, $A=0.5$ cm^2, $d=1$ μm, $\Delta_0^{\rm min}=2\times10^{-6}$ K, $\Delta_0^{\rm max}=4$ K, and $\Delta^{\rm max}=4$ K. Notice that the capacitance decays logarithmically with time in qualitative agreement with experiment. This logarithmic behavior depends on the fact that the TLS distribution $P(\Delta,\tilde{\lambda})$ is a constant. It is tempting to speculate that the logarithmic dependence arises from the TLS average over $\exp(-t/\tau_1)$, since this gives $\ln t$. However, the presence of other TLS factors in $\chi'_{2\pm}$ makes this far from obvious. Indeed, $\langle\chi''_{2\pm}\rangle_{\rm TLS}$ does not go simply as $\ln t$ even though

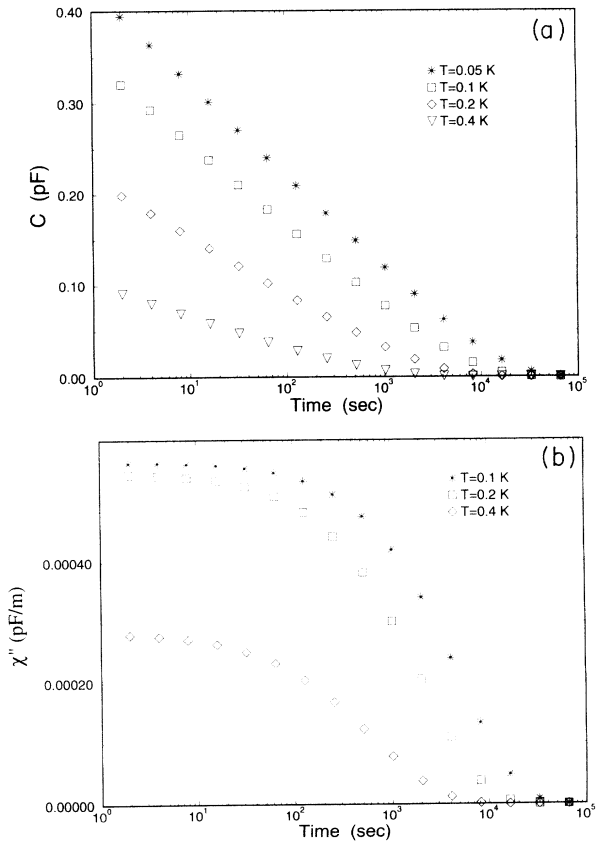

FIG. 1. (a) Capacitance versus $\ln t$ for various temperatures for noninteracting TLS. Only the contribution from $\chi'_{2\pm}$ is shown since this is the only term with time dependence. (b) $\chi''_{2\pm}$ versus $\ln t$ for various temperatures for noninteracting TLS. We have used the values for SiO_2: $\bar{P}=10^{32}$ erg^{-1}cm^{-3}, $\tilde{\gamma}=1$ eV, $\rho=2.2$ g/cm^3, $c_l=5.8\times10^5$ cm/s, $c_t=3.8\times10^5$ cm/s, $p_0=0.5$ Debye, $E_{\rm dc}=2\times10^6$ V/m, $A=0.5$ cm^2, $d=1$ μm, $\Delta_0^{\rm min}=2\times10^{-6}$ K, $\Delta_0^{\rm max}=4$ K, and $\Delta^{\rm max}=4$ K. We used $\Omega=2\pi\nu_{\rm ac}$ with $\nu_{\rm ac}=1$ kHz, though the curves do not change with frequency over the range of frequencies used experimentally.

$\chi''_{2\pm}$ has a factor of $\exp(-t/\tau_1)$. Using the same parameter values as in Fig. 1(a), we plot $\langle \chi''_{2\pm} \rangle_{\rm TLS}$ versus $\ln t$ for various temperatures in Fig. 1(b). We see that the curves are flat at short times. To understand this, note from Eq. (25) that the TLS with a short relaxation time τ_1 have large energy splittings $\hbar\omega_0 \gg \hbar\Omega$. This implies that the frequency-dependent terms in $\chi''_{2\pm}$ cancel, leaving a flat time-independent contribution from the TLS with small energy splittings and hence long relaxation times.

In Fig. 2, we plot the magnitude of the slope $|dC/d\ln t|$ versus temperature using the same parameters as in Fig. 1. We find that the temperature dependence of this relaxation rate agrees qualitatively with experiment when $p_0E \sim kT$. To understand this behavior, notice that the temperature affects the relative populations of the energy levels as expressed by terms such as $\tanh(\beta\epsilon/2)$ and $\tanh(\beta\bar{\epsilon}/2)$. At low temperatures where $kT < p_0E_{\rm dc}$, the jump in the capacitance will increase with decreasing temperature because the lower the temperature, the farther the initial population of the two-level systems is from the new equilibrium defined by the dc field. However, even though the jump increases, the slope does not change much with temperature at low temperatures. This disagrees with experiment which finds that the jump tracks the size of the slope. At high temperatures where $kT > p_0E_{\rm dc}$, the energy asymmetry introduced by the dc bias is relatively small, and the thermal population of the energy levels does not need to readjust very much. Hence the capacitance will not change much when the dc field is turned on, and the slope $(dC/d\ln t)$ will be close to zero. Thus the crossover from a finite slope at low temperatures to zero slope at high temperatures occurs at a temperature $kT \sim p_0E_{\rm dc}$. If we plug in numbers with the electric field $E \sim 2\times10^6$ V/m and dipole moment $p \sim 0.5$ D, which is the dipole moment of defects intrinsic to SiO_2,[16] then $p_0E \sim 200$ mK $\sim T$. The fact that the experiments are in the regime where $p_0E \sim kT$ is further confirmed by the sweeps of the dc field which find a hole in the capacitance at zero voltage. They also find that they can burn a hole by applying a given voltage to the sample for a while ($\sim$hours). As they raise the temperature the depth of the hole decreases. The width of the hole in volts can be defined as the width of the region which fills in with increasing T. The typical width of the hole in SiO_x is 10^6 V/m and the typical temperature at which the hole is diminished is $\sim$200 mK. The fact that the hole disappears at the typical experimental temperatures implies that $kT \sim p_0E$.

We also find that the noninteracting TLS model is consistent with a hole in the capacitance versus voltage. In Fig. 3 we have plotted the capacitance C versus $p_0E_{\rm dc}$ at $T=0.05$ K and $T=0.2$ K. In making this plot we have assumed that the system is in equilibrium at $E_{\rm dc}=0$ and that the dc field is swept infinitely fast. Thus we set $t=\infty$ for $E_{\rm dc}=0$, and $t=0$ at all nonzero voltages in Eq. (22). Here we assume that the dc field is turned on slowly enough to avoid inversion of the energy levels, i.e., we set $S_z^0(0) = -\tanh(\beta\epsilon/2)/2$. Notice that there is a hole centered at $p_0E_{\rm dc}=0$. This agrees qualitatively with experiment. Crudely speaking, the hole follows the thermal population factor $S_z^0(0) = -\tanh(\beta\epsilon/2)/2$ found in Eq. (22). This factor tells us that when $\epsilon \ll 2kT$, the TLS energy levels are equally populated and will not respond strongly to the ac field. On the other hand, when $\epsilon \gg 2kT$, the lower level will have a greater probability of being populated than the upper level and the response will be greater.

While experiment and two-level system theory agree, at least qualitatively, on the time, voltage, and temperature dependence, they disagree about the frequency dependence of the slope of the logarithmic time decay. The theory of noninteracting TLS says there is no frequency dependence, while experimentally the slope decreases roughly logarithmically with frequency. The reason why a noninteracting TLS model has no frequency dependence is because the experimental frequencies Ω, which are on the order of kHz, are much smaller than the typical effective energy splitting $\bar{\epsilon}$, which are on the order of GHz. This can be seen in Eq. (22) where the contribution of Ω is negligible because $\omega_0 \gg \Omega$. If we include TLS with such small energy splittings that $\omega_0 \sim \Omega$ by reducing $\Delta_0^{\rm min}$, then the magnitude of the jump in the capacitance

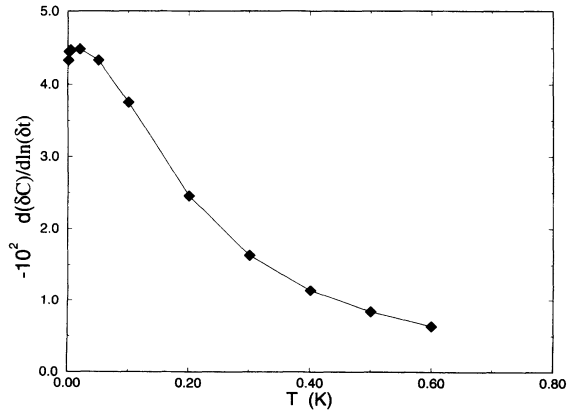

FIG. 2. Magnitude of the slope $|dC/d\ln t|$ versus temperature for noninteracting TLS. The parameters are the same as those used in Fig. 1.

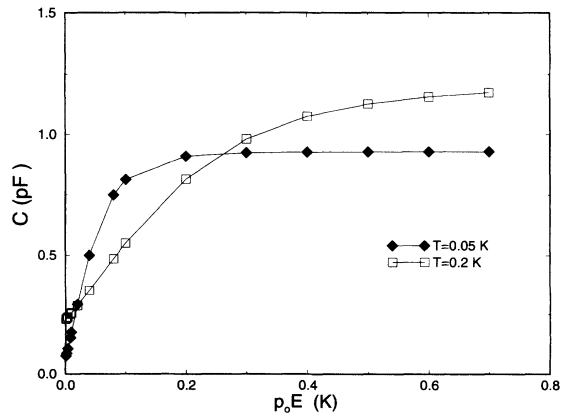

FIG. 3. Capacitance versus $p_0E_{\rm dc}$ for noninteracting TLS. The capacitance has been calculated using $\chi'_{1\pm}$, $\chi'_{2\pm}$, and χ'_z. The parameters are the same as those used in Fig. 1.

becomes frequency dependent, but the slope remains frequency independent. This is because TLS with such small energy splittings have very long τ_1's and decay very slowly [see Eq. (29)]. They essentially contribute a constant to the capacitance until they decay. (For a TLS with $\Delta=0$ and $\Delta_0^{\min}=2\times10^{-10}$ K, $\tau_1\sim10^{12}$ sec at 50 mK. Note that a small value for Δ_0 corresponds to a large barrier height which is physically reasonable.)

These long-lived TLS can experience a population inversion due to level crossing which will cause the capacitance at long times to fall below the value it had before the dc field was applied. As a result the theory of independent TLS predicts the change in capacitance due to the dc field to be positive at first and then to have a negative dip at longer times. As we mentioned earlier, when $\Delta\tilde{\Delta}<0$, $S_z^0(0)=(-\tanh(\beta\epsilon/2)/2)\times\mathrm{sgn}(\Delta\tilde{\Delta})$ can change sign, indicating population inversion. If the condition $\Delta\tilde{\Delta}<0$ is satisfied, then an estimate of the probability P_{zener} for such an inversion to occur is given by the Landau-Zener tunneling probability[17]

$$P_{\text{zener}}\sim\exp-\frac{\Delta_0^2\tau_r\pi}{2p_0E\hbar}\ , \tag{31}$$

where τ_r is the time it takes for the dc field E to rise to its final value. (The prefactor is of order unity.) This indicates that population inversion is appreciable when the exponent is small, i.e., when $\Delta_0\lesssim\sqrt{2\hbar p_0E/\tau_r\pi}$. In the case of the Stanford experiments, the rise time $\tau_r\sim100$ msec implies that $\Delta_0\sim3\times10^{-6}$ K if $E_{\text{dc}}=2\times10^6$ V/m. Setting $\Delta_0=\epsilon$ in Eq. (29) gives an upper bound for τ_1 of $\sim10^4$ sec at 50 mK. This indicates that the dip will occur about 10^4 sec after the dc field is applied. The fact that the negative dip is not seen experimentally, in spite of observation times as long as 8×10^4 sec, implies that the model of noninteracting two-level systems is not applicable, though the expression for P_{zener} in Eq. (31) is admittedly quite crude. From this expression for P_{zener}, we see that lowering τ_r and/or increasing the dc field E leads to the population inversion of TLS with larger Δ_0, and therefore smaller τ_1, so that the negative dip will occur earlier and be deeper. For example, if $\tau_r=10$ msec, ten times faster than in the current Stanford experiment, then $\Delta_0\sim10^{-5}$ K and $\tau_1\lesssim10^3$ sec at 50 mK. The corresponding time trace for the capacitance with $\Delta_0^{\min}\sim2\times10^{-10}$ K is shown in Fig. 4; the dip is clearly visible at time scales of order τ_1. It would be interesting to do a more systematic search for such a negative dip experimentally. Since we do not believe that interacting defects predicts such a dip, this would be a way of differentiating between interacting and noninteracting defects.

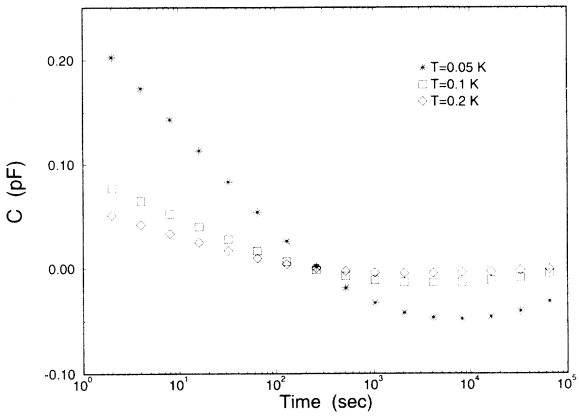

FIG. 4. Capacitance versus ln$t$ for noninteracting TLS. Only the contribution from $\chi'_{2\pm}$ is shown since this is the only term with time dependence. The parameters used are the same as for Fig. 1, except that $\Delta_0^{\min}=2\times10^{-10}$ K. Using this smaller value for $\Delta_0^{\min}$ implies that more TLS are being averaged over in Eq. (27). Notice the negative dip at long times produced by very slowly decaying TLS with inverted populations.

III. INTERACTING DEFECTS

The lack of agreement on the frequency dependence indicates that interactions between defects need to be included. The exact form of the interactions is not crucial as long as randomness is included. Thus we shall see that a very simple system which has both randomness and interactions, namely a nearest-neighbor Ising spin glass, gives qualitative agreement with experiment. Still, it is worth taking a moment to discuss the nature of the interactions in insulating glasses.

Since the dominant interaction between defects is mediated by the strain field, we start by considering defects with internal degrees of freedom that couple linearly to the strain field:

$$H=\sigma_{\alpha\beta}(r)\varepsilon_{\alpha\beta}(r), \tag{32}$$

where $\varepsilon_{\alpha\beta}(r)$ is the symmetric strain field and $\sigma_{\alpha\beta}(r)$ is the stress field associated with the defects. The indices α and β range over the real-space directions, x, y, and z and the sum over repeated indices is understood. As in the two-level system model of glasses,[1,2] we assume that the defects have internal degrees of freedom. Thus $\sigma_{\alpha\beta}$ can be replaced by $\Gamma_{\alpha\beta}\cdot\mathbf{S}$ where $\mathbf{S}$ is a spinlike TLS operator represented by Pauli matrices. $\Gamma_{\alpha\beta}$ is a vector in spin space and a matrix in real space. The spin representation is that of the energy eigenstates of the two-level system. S_x and S_y are operators for transitions between energy levels, while S_z does not involve transitions and is Ising-like.

The defects interact with each other via the strain field. First let us consider the effective S_zS_z interaction which does not involve transitions between energy levels. Using either elasticity theory[5] or second-order[3,18] perturbation theory to eliminate the strain field yields:

$$H_{\text{eff}}(\mathbf{r}-\mathbf{r}')=-\sum_{\lambda,\mathbf{k}}\frac{1}{\rho v_\lambda^2}\cos[\mathbf{k}\cdot(\mathbf{r}-\mathbf{r}')]\times\eta_{\alpha\beta}^{(\lambda)}\eta_{\gamma\delta}^{(\lambda)}\sigma_{\alpha\beta}(\mathbf{r})\sigma_{\gamma\delta}(\mathbf{r}')\ , \tag{33}$$

where $\eta_{\alpha\beta}^{(\lambda)}=(\hat{k}_\alpha\hat{e}_\beta^{(\lambda)}+\hat{k}_\beta\hat{e}_\alpha^{(\lambda)})/2$. The sum over λ is over the longitudinal and transverse phonon polarizations. ρ is the density and v is the speed of sound. $\hat{k}_\alpha$ is the αth component of the unit phonon wave vector and $\hat{e}_\beta$ is the βth component of the unit phonon polarization vector.

Summing over $\mathbf{k}$ is straightforward but tedious. Rather than writing out the result, we will simply comment on some of its features. Equation (33) is the tensor analog of a vector dipole-dipole interaction. It roughly goes as $g/|\mathbf{r}-\mathbf{r}'|^3$ where $g\sim\gamma^2/\rho v^2$ and γ is the order of magnitude of the defect stress. Taking $\gamma\sim 0.5$ eV, we estimate $g\sim 10^4$ K Å^3 for amorphous SiO_2.[3] Notice that this is an order of magnitude larger than the electrostatic interaction between two electric dipoles. A dipole moment of $\mu\sim 0.5$ D, which is the dipole moment of defects intrinsic to SiO_2,[16] gives $\mu^2\sim 10^3$ K Å^3. The interaction (33) does not change sign as the radial distance $|\mathbf{r}-\mathbf{r}'|$ changes, but it can change sign as the angular position of the defects changes due to terms which are proportional to $\delta_{ik}\hat{r}_j\hat{r}_l\sigma_{ij}(\mathbf{r})\sigma_{kl}(\mathbf{r}')$ and $\hat{r}_i\hat{r}_j\hat{r}_k\hat{r}_l\sigma_{ij}(\mathbf{r})\sigma_{kl}(\mathbf{r}')$, where $\hat{r}_i$ is the ith component of the unit vector connecting the two defects. Since the defects have random positions, there will be both positive and negative interactions, just as in a dipolar spin glass.

Now let us consider the effect of including transitions between energy levels, e.g., S_xS_x terms. Using second-order perturbation theory to calculate the effective interaction between two defects with energy splittings ΔE and $\Delta E'$, we find

$$H_{\text{eff}}(\mathbf{r}-\mathbf{r}')=\sum_{\lambda,\mathbf{k}}\frac{1}{2\rho v_\lambda^2}\left[\frac{v_\lambda^2k^2}{(\Delta E)^2-v_\lambda^2k^2}+\frac{v_\lambda^2k^2}{(\Delta E')^2-v_\lambda^2k^2}\right]\times\cos[\mathbf{k}\cdot(\mathbf{r}-\mathbf{r}')]\eta_{\alpha\beta}^{(\lambda)}\eta_{\gamma\delta}^{(\lambda)}\sigma_{\alpha\beta}(\mathbf{r})\sigma_{\gamma\delta}(\mathbf{r}')\ . \tag{34}$$

Notice that this reduces to Eq. (33) when $\Delta E=\Delta E'=0$. Summing over $\mathbf{k}$ yields oscillatory factors such as $\sin(\Delta E\cdot|\mathbf{r}-\mathbf{r}'|/v)$ and $\cos(\Delta E\cdot|\mathbf{r}-\mathbf{r}'|/v)$. This is the analog of Ruderman-Kittel-Kasuya-Yosida interactions which oscillate as a function of the distance $|\mathbf{r}-\mathbf{r}'|$. Equation (34) also has angular factors which vary in sign according to the placement of the defects and their orientation. As before, random positions of the defects result in interactions of random sign. Thus the system is the tensor analog of a spin glass.

The idea that an insulating glass can act like a spin glass is reinforced by recent experiments done by Fenimore and Weissman on a real spin glass (CuMn).[19] They have done the magnetic analog of the Stanford dielectric experiments and find similar results. For example, they find a hole in χ'' versus magnetic field H with the minimum being at the field in which the sample was cooled. They also find that χ'' relaxes logarithmically in time when they change the applied field from $+\mathbf{H}$ to $-\mathbf{H}$.

While we could use the previous discussion to justify modeling insulating glasses as spin glasses, we believe that it is important to point out that the exact form of the interactions is not crucial in explaining the experiments. In fact we can obtain qualitative agreement with experiment using an interacting Hamiltonian that is much simpler than the one in Eqs. (33) and (34). In general, interactions have two consequences: (1) they imply that clusters of defects behave as dynamical entities; and (2) they produce a hole in the distribution of local fields. We now discuss these two effects.

As we mentioned before, in order to explain the frequency dependence of the dielectric experiments, interactions must be included. Interactions lead to clusters of strongly interacting defects which make the capacitance frequency dependent. At low frequencies large slow clusters as well as small fast clusters contribute to the response, while at high frequencies only small fast clusters have time to respond. This is consistent with the experimental observation of the jump in the capacitance being bigger and the slope $|dC/d\ln t|$ being larger at low frequencies than at high frequencies.

Interactions also prevent the distribution of local fields at defect sites from being flat. In particular, stability arguments have been used to show that there must be a hole in the distribution of local fields.[20,21] To be more specific, think of a spin glass with long-range interactions.[20] Suppose you find the ground-state spin configuration and suppose that the distribution of local magnetic fields $P(h)$ is finite at $h=0$. This means that those spins with no local field can flip without changing their energy. But if they do so, other spins have their field altered and so some of them will flip. This in turn causes others to flip and so on. This avalanche means that the supposed ground state is not stable. In order to have a stable ground state, the distribution of local fields must go to zero as the local field $h\to 0$.

The Stanford experiments are the first to test these long standing ideas about a hole in the local-field distribution of glasses because the strong dc field enables them to probe $P(h)$ away from $h=0$. Consider the situation before the application of the dc field. Defects whose local fields are small can flip easily in response to the ac field; these are the main contributors to the capacitance. In fact, we can show that the electric susceptibility due to single Ising dipoles is proportional to $P(0)$. Consider an Ising spin glass in a magnetic field:

$$H=H_0-S_zh_z(t)\ , \tag{35}$$

where the field $h_z(t)=h+h_1\cos\Omega t$ acts on an Ising spin $S_z=\pm\frac{1}{2}$ and h is a constant field. The thermal average of the spin $[S_z]_{\text{th}}=\tanh(\beta h_z(t)/2)/2$. Expanding this to lowest order in h_1, we obtain

$$[S_z]_{\text{th}}\simeq\frac{1}{2}\tanh\frac{\beta h}{2}+\frac{\beta h_1}{4}\left[1-\tanh^2\left[\frac{\beta h}{2}\right]\right]\cos\Omega t\ . \tag{36}$$

The susceptibility χ' in phase with the ac field is given by

$$\chi'(h)=2\left[\frac{d\langle[S_z]_{\text{th}}\cos\Omega t\rangle}{dh_1}\right]_{h_1=0}=\frac{\beta}{4}\left[1-\tanh^2\left[\frac{\beta h}{2}\right]\right], \tag{37}$$

where $\langle\ldots\rangle$ denotes an average over one period. The factor of 2 cancels the factor of $\frac{1}{2}$ that comes from $\langle\cos^2\Omega t\rangle$. In a random system we must average over the distribution of local fields $P(h)$. Thus the disorder average is

$$\langle \chi' \rangle_{\rm dis} = \int_{-\infty}^{\infty} dh\, P(h)\chi'(h) \ . \tag{38}$$

If we assume that only the spins with a small local-field contribute, then we can replace $P(h)$ with $P(0)$. Thus

$$\langle \chi' \rangle_{\rm dis} \simeq P(0) \int_{-\infty}^{\infty} dh\, \chi'(h) = P(0) \ . \tag{39}$$

This contribution dominates the susceptibility at low temperatures and high frequencies. When the dc field is applied, a new set of defects find themselves in zero local field. The applied dc field effectively shifts the local-field distribution along the local-field axis. Immediately after the dc field is switched on, $P(0)$ will be large and finite. Thus the susceptibility and hence capacitance suddenly jumps up. The size of the jump increases with the depth of the old hole out of which the system jumps. Since the hole is smeared by thermal effects, we expect that the size of the jump will increase as the temperature decreases. Once the dc field is switched on, a new hole develops and the capacitance decreases with time.

We can test these ideas about the effects of interactions by studying a simple system that incorporates both randomness and interactions. The three-dimensional nearest-neighbor Ising spin glass is just such a system. We have performed heat-bath Monte Carlo simulations on this system. The spins represent the interacting electric dipoles in the glass samples. We place the spins on the sites of a cubic lattice of size 10^3, and choose the exchange interactions from a Gaussian distribution centered at zero with a variance of unity. This system is known to have a transition temperature of about 0.9.[22] We have run at temperatures ranging from 0.1 to 0.9. In order to simulate the conditions of the experiment, we run for $N/2$ Monte Carlo steps per spin with no applied field, then switch on a dc field ($p_0 E_{\rm dc} \sim 0.4$ and $p_0 = 1$) and run for another $N/2$ Monte Carlo steps, where N is the total number of Monte Carlo steps. We used $N = 12\,000$ and 25 000 Monte Carlo steps. We need not achieve complete thermal equilibrium at low temperatures since we are interested in nonequilibrium phenomena. To average over the disorder, we averaged up to 8000 samples.

To measure the susceptibility, a small ac field $E_{\rm ac}\cos\Omega t$ is applied with an amplitude $E_{\rm ac} \sim 0.03$ and an oscillation period between 4 and 128 times steps. (A pass through the lattice takes one time step.) By measuring the polarization $M(t)$ as a function of time, we can deduce the susceptibility which is proportional to the capacitance.

$$\chi' = 2\frac{\langle M(t)\cos\Omega t \rangle}{E_{\rm ac}} = \frac{2}{\tau_0 E_{\rm ac}} \sum_{i=1}^{\tau_0} M(t_i)\cos\Omega t_i \ , \tag{40}$$

$$\chi'' = 2\frac{\langle M(t)\sin\Omega t \rangle}{E_{\rm ac}} = \frac{2}{\tau_0 E_{\rm ac}} \sum_{i=1}^{\tau_0} M(t_i)\sin(\Omega t_i + \phi) \ , \tag{41}$$

where we are averaging over a period τ_0. The factor of 2 cancels the factor of $\frac{1}{2}$ that comes from $\langle \cos^2\Omega t \rangle$ or $\langle \sin^2\Omega t \rangle$. The phase factor ϕ is used to cancel spurious effects from a linear relaxation. In other words, if $M(t)$ decreases linearly in time but does not respond to the ac field, we would get a spurious response in χ'' if we simply do the average $\langle M(t)\sin\Omega t \rangle$ with $\phi = 0$. An appropriately chosen ϕ cancels out this effect.

The results of our simulations show that the application of a dc field causes the capacitance to jump up and then decay logarithmically with time as shown in Fig. 5(a). [Figure 5(b) shows the behavior of the imaginary

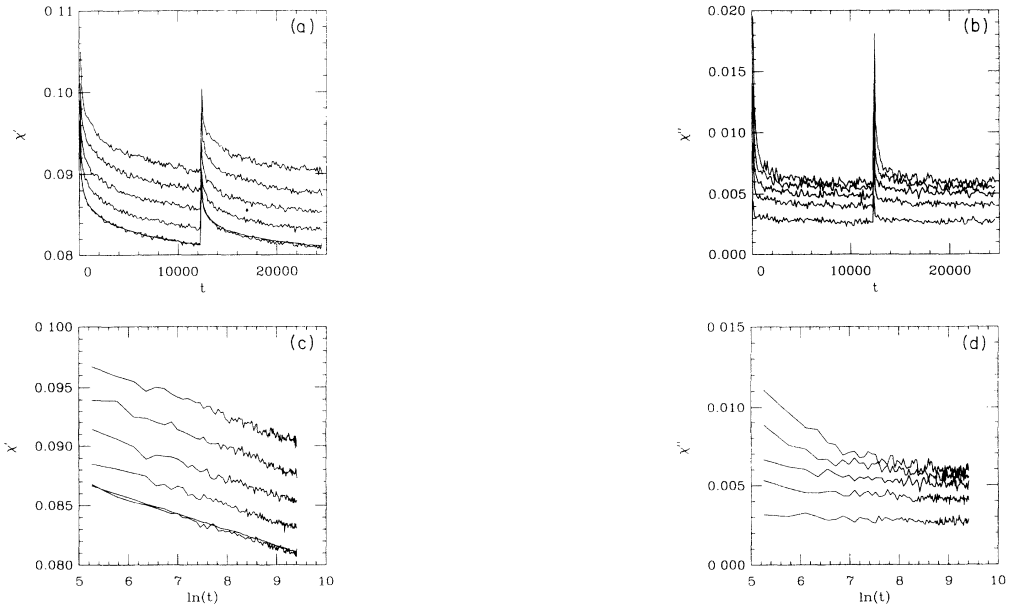

FIG. 5. χ' and χ'' vs time in Monte Carlo steps (MCS) per spin at different frequencies from nearest-neighbor Ising spin-glass simulations. From top to bottom the periods of the ac field are 64, 32, 16, 8, and 4 MCS per spin. 8000 samples were averaged over and $T = 0.1$. The rather smooth solid line in the χ' plots that goes through the highest frequency (shortest period) curve is $P(0)$. Note that $P(0)$ is independent of frequency. (c) and (d) show the same data as (a) and (b) but plotted vs ln$t$. Notice that χ' has logarithmic time dependence.

part of the susceptibility.] We also monitor the hole in the local-field distribution and find that $P(0)$ matches the susceptibility at the highest frequency, indicating that the high-frequency response is due primarily to single spin flips. Note that $P(0)$ is less than the low-frequency susceptibility, which indicates that the single spin flips are joined by somewhat slower clusters of spins in contributing to the time-dependent capacitance at low frequencies. Because of these clusters, the Monte Carlo simulations see qualitatively the correct frequency dependence of the logarithmic slope of the decay as shown in Fig. 6. However, experimentally the slope $|dC/d\ln t|$ decreases by a factor of 5 as the frequency increases from 300 Hz to 30 kHz, while the simulations only show a decrease in slope by a factor of 2. This is because the clusters responding in the real glass are much bigger than those in the simulation. There are two reasons for this. First, the response measured by the real part of the susceptibility involves all clusters whose frequencies are less than or equal to the ac frequency. Since the ratio of the microscopic frequencies to the ac frequencies is much larger in the experiment than in the simulation, the experiment is able to measure the response from much bigger clusters than is the simulation. Second, the experimental sample contains many more defects than the system in the simulation. However, since the typical spacing of TLS with energy splittings less than or of order 200 mK is 1000 Å in a real glass, our Ising spin glass with 10^3 spins represents a 1-μm^3 sample.

Figure 6 also indicates the fluctuations in our results by showing two curves that differ in the number of samples, the number of Monte Carlo steps, and their bond configurations. The difference between the two curves comes from the fact that we are taking a second derivative, i.e., the slope is roughly $d^2M/dE_{ac}d\ln t$. Derivatives are quite sensitive to numerical noise. For example, the noise in the time traces in Fig. 5 leads to some error

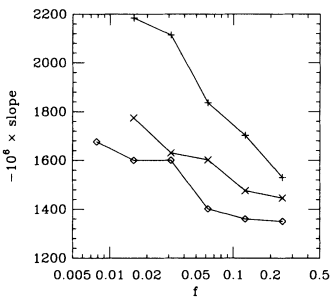

FIG. 6. Magnitude of the slope $|d\chi'/d\ln t|$ versus frequency f, where f is the inverse of the period in Monte Carlo steps (MCS) per spin. The slope has been multiplied by a factor of 10^6. The top curve (+) was done at $T=0.2$ with 4000 samples and $N=12\,000$ MCS per spin. The middle curve (×) was done at $T=0.1$ with 4000 samples and $N=12\,000$ MCS per spin. The bottom curve (◇) was done at $T=0.1$ with 8000 samples and $N=25\,000$ MCS per spin. The same bond configuration was used for the curves averaged over 4000 samples, but a different bond configuration was used for the 8000 sample curve. Comparing the bottom two curves gives some idea of the fluctuations resulting from taking the second derivative $\approx d^2M/dE_{ac}d\ln t$, where M is the polarization.

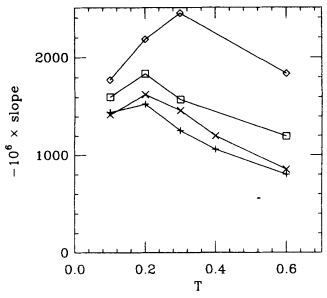

FIG. 7. Magnitude of the slope $|d\chi'/d\ln t|$ versus temperature T at different frequencies. The slope has been multiplied by a factor of 10^6. $f=1/64$ MCS per spin (◇), $f=\frac{1}{16}$ MCS per spin (□), and $f=\frac{1}{4}$ MCS per spin (+). The second curve from the bottom (×) represents $P(0)$ which is independent of frequency. Each point represents an average over 4000 samples with 12 000 MCS per spin. The same bond configuration was used for all the data.

in defining the slopes of these curves. Thus, it is the qualitative trends rather than the absolute values that are significant in Figs. 5–7. To reduce the scatter in the data, we have used the same bond configurations in Figs. 5 and 7.

In Fig. 7, we show the magnitude of the logarithmic slope versus temperature for $P(0)$ and for χ' at different frequencies. Although there is a slight initial increase at low temperature, the slope decreases with increasing temperature when $kT\sim p_0E$ for the reasons we discussed before. We only achieve qualitative agreement with experiment because the clusters are smaller in the simulation than in real samples, and because $P(0)$ in the nearest-neighbor Ising spin glass does not go to zero at $T=0$, while it does in a system which has long-range interactions.

IV. TWO-LEVEL SYSTEMS AND $P(0)$

In order to sort out the role of single defects versus clusters, we have combined the two-level system contribution to the capacitance with the hole in the density of states required by stability arguments. In particular, the results of the Bloch equations for individual two-level systems shows that the susceptibility χ' can be written as the sum of three pieces; $\chi'_z(\Omega,T)$ in Eq. (20) depends on frequency and temperature but is independent of time; $\chi'_{1\pm}(T)$ in Eq. (21) depends on temperature but not time or frequency; and $\chi'_{2\pm}(t,T)$ in Eq. (22) depends on time and temperature but not on frequency. Notice that $\chi'_{1\pm}(T)$ and $\chi'_{2\pm}(t,T)$ have no frequency dependence because $\Omega\ll\omega_0$, while $\chi'_z(\Omega,T)$ has frequency dependence because the product $\tau_1\Omega$ in the denominator can be large. If we average $\chi'_z(\Omega,T)$ over a time-dependent density of states, then the capacitance would have both time and frequency dependence.

To accomplish this, we model the TLS density of states $P(E)$ as a step function, i.e., the density of states has a hole in the shape of a square well. Since the width of the hole is comparable the temperature, we set $P(E)=P(0)$ for $E\lesssim kT$ and $P(E)=\bar{P}$ for $E\gtrsim kT$. As we saw in Fig. 5, $P(0)$ can be time dependent. In particular, immediate-

ly after the dc field is applied, $P(0)$ initially equals $\bar{P}$, but then decreases as the hole develops. Our Ising spin-glass simulations indicate that $P(0)$ decreases logarithmically in time in qualitative agreement with the experimentally observed time dependence of the capacitance. We can write $P(0)$ as the sum of the constant density of states $\bar{P}$ and the developing hole in the density of states at low energies $\Delta P(t,T)$.

$$P(0)=\bar{P}+\Delta P(t,T) \tag{42}$$

$\Delta P(t,T)$ depends on T because the growth of the hole may be a function of temperature.

In the average over the distribution of two-level systems, the principal contribution to the response comes from dipoles with very small local fields. Thus we can replace the usual constant density of states $\bar{P}$ by $P(0)$ in Eq. (27). Since the time dependence of the capacitance comes from the time dependence of the hole whose width is of order kT, we set $\Delta_0^{\max}=\Delta^{\max}=kT$. Averaging $\chi_z'(\Omega,T)$ over TLS using $P(0)$ leads to a contribution to the capacitance that has frequency, time, and temperature dependence. We assume that on the time scale of the experiment $(0\le t\lesssim 10^6)$, $\Delta P(t,T)=-P_1\ln[(t+t_0)/t_0]$ where the dc field is applied at $t=0$, t_0 is of order a few seconds, and P_1 is such that $P(0)\sim 0$ at $t\sim 10^6$ seconds. Since $\Delta P(t,T)$ has logarithmic time dependence, the equilibrium capacitance $C_{\rm eq}$, which comes from $\langle\chi_z'\rangle_{\rm TLS}+\langle\chi_{1\pm}'\rangle_{\rm TLS}$, gives the slope, i.e., the coefficient of $\ln t$.[23] We plot this slope in Fig. 8. Notice that the slope decreases with increasing frequency Ω. Eventually, at high enough frequencies, $\chi_{1\pm}'$ dominates and the slope becomes independent of frequency. As Fig. 8 indicates, we estimate that the decrease in slope between 100 and 10^4 Hz is at most a factor of 2, which is less than the factor of 5 seen experimentally. This implies that clusters play an important role in the frequency dependence of the capacitance. To the best of our knowledge, these experiments are the first to indicate that clusters are important in understanding the dynamics of glasses. This lack of agreement in the frequency dependence does not mean that the hole in the distribution of local fields is unimportant. Clusters also have distributions of local fields and these have holes at $h=0$ due to stability arguments. These holes contribute to the observed hole in the dc voltage sweeps of the capacitance.[24]

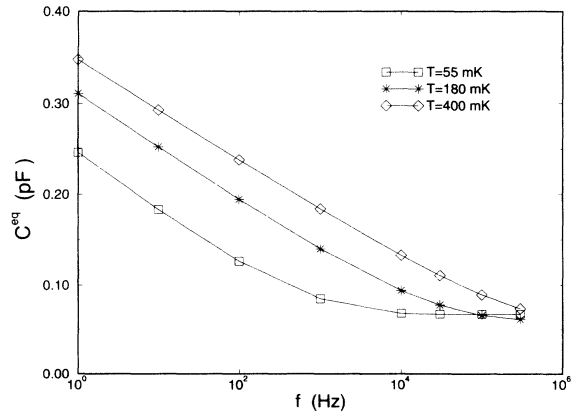

FIG. 8. The equilibrium capacitance (pF) vs frequency (Hz) for TLS. The capacitance is calculated using χ_z' from Eq. (20) and $\chi_{1\pm}'$ from Eq. (21). We averaged over the TLS parameters used for Fig. 1 but with $\Delta_0^{\max}=\Delta^{\max}=kT$. If we consider $P(0)$ to have logarithmic time dependence, then $C_{\rm eq}$ represents the "slope", i.e., the coefficient of $\ln t$. Notice that in the experimental range between 10^2 and 10^4 Hz, the $C_{\rm eq}$ varies by at most a factor of 2.

In Fig. 8, notice that $C_{\rm eq}$ increases with increasing temperature. This is due to the fact that the temperature dependence of χ_z' is dominated by the temperature dependence of τ_1 [see Eq. (20)]. Since $\tau_1\sim T^{-1}$ for $\beta\tilde{\epsilon}\ll 1$ [see Eq. (29)], $\chi_z'\sim T$ for TLS with small Δ_0. (τ_1 is dominated by small Δ_0.) From Fig. 8, we see that this tendency to increase with increasing temperature survives averaging over TLS. Although the resulting temperature dependence disagrees with that found experimentally for the slope, we have neglected the temperature dependence of $\Delta P(t,T)$ which could change this.

V. CONCLUSIONS

To summarize, we have analyzed recent nonlinear dielectric experiments in which large dc fields are applied to capacitors with glass dielectrics. The capacitance jumps up and then decays logarithmically with time. While we can explain the jump and subsequent decay with independent two-level systems, we cannot explain the observed frequency dependence with the independent TLS model which predicts no frequency dependence because the ac frequency is much less than the effective TLS energy splitting. Thus we must include interactions between defects. Interactions lead to cluster formation as well as a hole in the local-field distribution. We have observed both of these effects in Monte Carlo simulations of the nearest-neighbor Ising spin glass in three dimensions. The hole in the local-field distribution is consistent with the hole observed in the dc field sweeps of the capacitance. However, we conclude that the rather large frequency dependence of the slope $|dC/d\ln t|$ indicates that clusters of defects play an important role in the dielectric response. In particular large slow cluster are able to participate at low frequencies but not at high frequencies.

One way to check experimentally that interacting, rather than noninteracting, defects are the correct description of glasses would be to study the capacitance as a function of time for very long times after the dc field has been applied. As we discussed earlier, the model of independent TLS predicts that the capacitance will fall below its pre-dc field value, while the scenario involving the hole in the distribution of local fields predicts that the capacitance will never fall below the value it had before the dc field was applied.

Still, we are left with the following question: if interactions are so important, why do noninteracting two-level systems work as well as they do in explaining equilibrium low-temperature experiments? There are two possible explanations. The first is that there are domains or clusters of interacting defects. These clumps of defects will have randomly spaced energy levels with random matrix ele-

ments connecting them and allowing transitions.[3] At low temperatures the low-lying energy levels will dominate and act like "two-level systems." Another way to reconcile interactions and two-level systems was proposed by Coppersmith[7] who assumes that the defects are strongly interacting tunneling centers. Strong interactions suppress tunneling in most of the defects, but for a few of the defects, the interactions from their neighbors cancel out to a large extent, leaving these defects free to tunnel. In this scenario it is these "fully frustrated" defects which are the observed two-level systems. Since independent defects are unable to describe the frequency dependence of the nonequilibrium dielectric experiments, it would seem that this latter scenario is not the whole story and that further investigation of the cluster picture is warranted.

ACKNOWLEDGMENTS

We would like to thank Doug Osheroff, Sven Rogge, Dom Salvino, Ben Tigner, and Tony Leggett for helpful discussions. ERG and CCY were supported in part by ONR Grant No. N000014-91-J-1502 and Los Alamos National Laboratory, and HMC acknowledges support from NSF Grant No. DMR-9214236. CCY thanks the Alfred P. Sloan Foundation for financial support.

*Current address: Department of Physics, U. of California, Irvine, Irvine, CA 92717.

†Current address: Lehman Brothers Inc., New York, NY 10285-0700.

[1]Good reviews are *Amorphous Solids,* edited by W. A. Phillips (Springer, Berlin, 1981); and S. Hunklinger and A. K. Raychaudhuri, Prog. Low Temp. Phys. **9**, 265 (1986).

[2]W. A. Phillips, Rep. Prog. Phys. **50**, 1657 (1987) is another good review.

[3]C. C. Yu and A. J. Leggett, Commun. Condens. Mater. Phys. **14**, 231 (1988); C. C. Yu, Phys. Rev. Lett. **63**, 1160 (1989); **69**, 2787 (1992).

[4]M. W. Klein, Phys. Rev. B **45**, 5209 (1992); M. W. Klein, Phys. Rev. Lett. **65**, 3017 (1990); M. P. Solf and M. W. Klein, Phys. Rev. B **46**, 8147 (1992); **47**, 11 097 (1993); **49**, 12 703 (1994).

[5]E. R. Grannan, M. Randeria, and J. P. Sethna, Phys. Rev. Lett. **60**, 1402 (1988); Phys. Rev. B **41**, 7784; 7799 (1990).

[6]S. V. Maleev, Sov. Phys. JETP **67**, 157 (1988); A. L. Burin, JETP Lett. **54**, 320 (1991); and D. A. Parshin, Phys. Rev. B **49**, 9400 (1994).

[7]S. N. Coppersmith, Phys. Rev. Lett. **67**, 2315 (1991).

[8]B. Tigner, D. J. Salvino, S. Rogge, and D. D. Osheroff, *Phonon Scattering in Condensed Matter VII,* edited by M. Meissner and R. O. Pohl (Springer-Verlag, Berlin, 1993), p. 285; S. Rogge, D. J. Salvino, B. Tigner, and D. D. Osheroff, in Proceedings of the 20th International Conference on Low Temperature Physics, Eugene, Oregon, 1993 [Physica B **194-195**, 407 (1994)]; and Phys. Rev. Lett. **73**, 268 (1994).

[9]D. J. Salvino, Ph.D. thesis, Stanford, 1993.

[10]In this case we can relate dipole moments to spin because we are considering a two-level system. In general, however, the two do not have the same dynamics because the dipole moment **p** is not conserved whereas the spin **S** is conserved.

[11]C. P. Slichter, *Principles of Magnetic Resonance,* 3rd ed. (Springer-Verlag, Berlin, 1990).

[12]S. Hunklinger and W. Arnold, in *Physical Acoustics: Principles and Methods,* edited by W. P. Mason and R. N. Thurston (Academic, New York, 1976), Vol. 12, p. 155.

[13]W. H. Press, S. A. Teukolsky, W. T. Vetterling, and B. P. Flannery, *Numerical Recipes: The Art of Scientific Computing,* 2nd ed. (Cambridge University Press, Cambridge, 1992), p. 155.

[14]B. Golding and J. E. Graebner, Phys. Rev. Lett. **37**, 852 (1986); and J. E. Graebner and B. Golding, Phys. Rev. B **19**, 964 (1979).

[15]L. Bernard, L. Piche, G. Schumacher, and J. Joffrin, J. Low Temp. Phys. **35**, 411 (1979).

[16]B. Golding, M. v. Schickfus, S. Hunklinger, and K. Dransfeld, Phys. Rev. Lett. **43**, 1817 (1979).

[17]E. Shimshoni and M. Gefen, Ann. Phys. **210**, 16 (1991).

[18]J. Joffrin and A. Levelut, J. Phys. (Paris) **36**, 811 (1976).

[19]P. W. Fenimore and M. B. Weissman, in Proceedings of the 6th Joint MMM-Intermag Conference, Albuquerque, New Mexico, 1994 [J. Appl. Phys. (to be published)].

[20]S. Kirkpatrick and C. M. Varma, Solid State Commun. **25**, 821 (1978).

[21]S. D. Baranovskiĭ, B. I. Shklovskiĭ, and A. L. Éfros, Zh. Eksp. Teor. Fiz. **78**, 395 (1980) [Sov. Phys. JETP **51**, 199 (1980)]; and A. L. Éfros and B. I. Shklovskiĭ, in *Electron-Electron Interactions in Disordered Systems,* edited by A. L. Éfros and M. Pollak (North-Holland, Amsterdam, 1985), p. 409.

[22]R. N. Bhatt and A. P. Young, Phys. Rev. B **37**, 5606 (1988).

[23]We neglect the convolution of $\chi'_{2\pm}$ and $\Delta P(t,T)$ because it is frequency independent and adds a constant to the capacitance that worsens the agreement with the experimental frequency dependence, though its time dependence will not be strictly logarithmic. Notice that at long times, $\chi'_{2\pm}$ is much smaller than $\chi'_{1\pm}$ and χ'_z due to the factor of $[S_z^0(0)-S_z^0(\infty)]e^{-t/\tau_1}$. Typically at $T=0.05$ K, $\langle\chi'_{2\pm}\rangle_{\rm TLS}\sim 6\times10^{-4}$ pF/m after applying the dc field for 8000 seconds, while $\langle\chi'_z\rangle_{\rm TLS}\sim 8\times10^{-3}$ pF/m and $\langle\chi'_{1\pm}\rangle_{\rm TLS}\sim 6\times10^{-3}$ pF/m.

[24]J. L. Black and B. I. Halperin, Phys. Rev. B **16**, 2879 (1977).